J|A|C|S
ARTICLES
Published on Web 12/01/2006

Chiral Alignment of OPV Chromophores: Exploitation of the Ureidophthalimide-Based Foldamer

Renatus W. Sinkeldam,[†] Freek J. M. Hoeben,[†] Maarten J. Pouderoijen,[†] Inge De Cat,[‡] Jian Zhang,[‡] Shuhei Furukawa,[‡] Steven De Feyter,[‡] Jef A. J. M. Vekemans,[†] and E. W. Meijer*[,†]

Contribution from the Laboratory of Macromolecular and Organic Chemistry, Eindhoven University of Technology, P.O. Box 513, 5600 MB Eindhoven, The Netherlands and Laboratory of Photochemistry and Spectroscopy, Division of Molecular and Nano Materials, Department of Chemistry, Katholieke Universiteit Leuven, Celestijnenlaan 200 F, B-3001 Leuven, Belgium

Received June 2, 2006; Revised Manuscript Received October 6, 2006; E-mail: E.W.Meijer@tue.nl

Abstract: The ability of foldamers to adopt a secondary structure in solution has been exploited to organize peripheral functionality. Our previously reported poly(ureidophthalimide) foldamer proved to be an excellent scaffold for the chiral organization of peripherally positioned oligo(*p*-phenylenevinylene) (OPV) chromophores. Facile high-yielding synthesis gave access to the required OPV-decorated building blocks. A condensation polymerization provided polymers of sufficient length to allow construction of a helical architecture comprising several turns. Short and long chains were separated by chromatography. Circular dichroism studies in THF of the longer chains indicate the presence of helically arranged OPVs. However, such an effect is not observed in $CHCl_3$. Remarkable are the measurements of the OPV foldamers in heptane. A bisignate Cotton effect is observed in heptane of a sample with a THF history. No Cotton effect is observed in heptane of a sample with a $CHCl_3$ history. In this example of supramolecular synthesis, the solvent dictates the expression of supramolecular chirality in a secondary structure. The short-chain oligomeric fractions that are unable to create a full turn revealed on scanning tunneling microscopy analysis the presence of circular architectures at the graphite/1-phenyloctane interface. This is in full agreement with the proposed conformation of the decorated foldamers.

Introduction

Research on foldamers was pioneered by Gellman et al.[1] and Moore et al.[2] for oligopeptides and abiotic, non-peptidomimetic oligomers, respectively. The first abiotic oligomer capable of folding was introduced by Hamilton et al. with his oligoanthranilamides,[3] rapidly followed by the first oligo(*m*-phenyleneethynylene) (*m*PE)[4] by Moore et al. The term "foldamer" is used to categorize dynamic oligomeric systems that are capable of folding into a conformationally ordered state in solution.[2] Through the years, the term was also used for structures that are preferentially held in a helical ordered state while the presence of a dynamic disordered state is less obvious. Since the beginning, a large variety of synthetic foldamers have been designed, each type utilizing a characteristic combination of secondary interactions to direct the folding or well-defined conformation.[5] A number of design strategies are prominent in recent literature. The folding of *m*PEs,[4,6] *o*PE,[7] and aromatic electron donor−acceptor couples[8] relies on solvophobic interactions in combination with $\pi-\pi$ stacking. Another class is represented by the aromatic oligoamides reported by Huc et al.,[9] Gong et al.,[10] and others,[11] where $\pi-\pi$ stacking is combined with hydrogen-bonding interactions to direct folding. The latter

[†] Eindhoven University of Technology.
[‡] Katholieke Universiteit Leuven.

(1) Appella, D. H.; Christianson, L. A.; Karle, I. L.; Powell, D. R.; Gellman, S. H. *J. Am. Chem. Soc.* **1996**, *118*, 13071−13072.
(2) Hill, D. J.; Mio, M. J.; Prince, R. B.; Hughes, T. S.; Moore, J. S. *Chem. Rev.* **2001**, *201*, 3893−4011.
(3) Hamuro, Y.; Geib, S. J.; Hamilton, D. A. *J. Am. Chem. Soc.* **1996**, *118*, 7529−7541.
(4) Nelson, J. C.; Saven, J. G.; Moore, J. S.; Wolynes, P. G. *Science* **1997**, *277*, 1793−1796.
(5) (a) Block, M. A. B.; Kaiser, C.; Khan, A.; Hecht, S. *Top. Curr. Chem.* **2005**, *245*, 89−150. (b) Sandford, A. R.; Yamato, K.; Yang, X.; Han, Y.; Gong, B. *Eur. J. Biochem.* **2004**, *271*, 1416−1425. (c) Huc, I. *Eur. J. Org. Chem.* **2004**, 17−29. (d) Schmuck, C. *Angew. Chem., Int. Ed.* **2003**, 2448−2452. (e) Gellman, S. H. *Acc. Chem. Res.* **1998**, *31*, 173−180.
(6) (a) Matsuda, K.; Stone, M. T.; Moore, J. S. *J. Am. Chem. Soc.* **2002**, *124*, 11836−11837. (b) Brunsveld, L.; Meijer, E. W.; Prince, R. B.; Moore, J. S. *J. Am. Chem. Soc.* **2001**, *123*, 7978−7984. (c) Prince, R. B.; Brunsveld, L.; Meijer, E. W.; Moore, J. S. *Angew. Chem., Int. Ed.* **2000**, *39*, 228−230. (d) Prince, R. B.; Saven, J. G.; Wolynes, P. G.; Moore, J. S. *J. Am. Chem. Soc.* **1999**, *121*, 3114−3121.
(7) (a) Jones, T. V.; Blatchly, R. A.; Tew, G. N. *Org. Lett.* **2003**, *5*, 3297−3299. (b) Blatchly, R. A.; Tew, G. N. *J. Org. Chem.* **2003**, *68*, 8780−8785.
(8) Nguyen, J. Q.; Iverson, B. L. *J. Am. Chem. Soc.* **1999**, *121*, 2639−2640.
(9) (a) Dolain, C.; Jiang, H.; Léger, J. M.; Guionneau, P.; Huc, I. *J. Am. Chem. Soc.* **2005**, *127*, 12943−12951. (b) Berl, V.; Huc, I.; Khoury, R. G.; Lehn, J. M. *Chem.−Eur. J.* **2001**, *7*, 2798−2809.
(10) (a) Yuan, L.; Zeng, H.; Yamato, K.; Sanford, A. R.; Feng, W.; Atreya, H. S.; Sukumaran, D. K.; Szyperski, T.; Gong, B. *J. Am. Chem. Soc.* **2004**, *126*, 16528−16537. (b) Yang, Z.; Yuan, L.; Yamato, K.; Brown, A. L.; Feng, W.; Furukawa, M.; Zeng, X. C.; Gong, B. *J. Am. Chem. Soc.* **2004**, *126*, 3148−3162.
(11) (a) Hunter, C. A.; Spitaleri, A.; Tomas, S. *Chem. Commun.* **2005**, 3691−3693. (b) Tanatani, A.; Yokoyama, A.; Azumaya, I.; Takakura, Y.; Mitsui, C.; Shiro, M.; Uchiyama, M.; Muranaka, A.; Kobayashi, N.; Yokozawa, T. *J. Am. Chem. Soc.* **2005**, *127*, 8553−8561. (c) Hamuro, Y.; Geib, S. J.; Hamilton, A. D. *J. Am. Chem. Soc.* **1997**, *119*, 10587−10593.

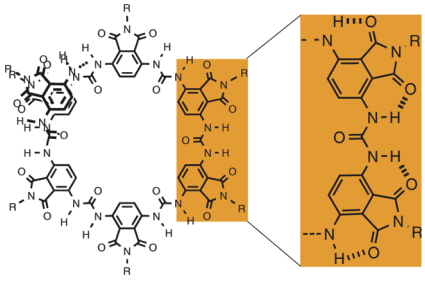

Figure 1. Poly(ureidophthalimide)s and a detailed hydrogen-bonding unit.

class is described in more detail in recent reviews.[12] Less common is the design based on oligo(aromatic urea)s: whereas the ones reported by Gong et al.[13] are present in a cisoid conformation, those of Zimmerman et al.[14] are forced in a transoid conformation due to intramolecular hydrogen bonding. Recently, we presented a helical foldamer based on poly(ureidophthalimide)s in which the urea linker adopts a cisoid conformation due to intramolecular hydrogen bonding (Figure 1).[15] Similar to the oligoamides, these poly(aromatic urea)s use intramolecular hydrogen bonding to direct folding. Molecular modeling studies[16] as well as an X-ray structure of a representative dimer[17] strongly support the curved and coplanar conformation of the backbone. This curvature will lead to a helical arrangement for longer oligomers with lengths exceeding 7−9 units, where it is proposed that $\pi-\pi$ interactions further stabilize the helical architecture once a turn is completed.

A potentially interesting function for helical foldamers is the exploitation of the inner void to host a guest. Depending on the design, helical foldamers may possess an inner void of sufficient size to accommodate ions[18] or small molecules.[19−21] The efforts of this research may eventually lead to synthetic trans-membrane ion channels.[9b] In addition to the exploitation of the inner void, the helical architecture may also be a promising candidate for the organization of peripheral functionality. To the best of our knowledge, this opportunity has not yet been addressed. Alignment of chromophores is of interest in the field of molecular electronics such as organic photovoltaics[22] and organic field effect transistors.[23] In this article, we report foldamers that utilize the periphery to align oligo(*p*-phenylenevinylene) (OPV) chromophores in a chiral fashion. We chose to decorate the previously reported poly(ureidophthalimide)[15] with OPVs since this type of chromophore has been studied in great detail in supramolecular homo-assemblies[24] and hetero-assemblies.[25] Furthermore, the large π-system of OPV chromophores may help to stabilize the helical architecture. Recently, we reported a general synthetic strategy to obtain an array of 3,6-diaminophthalimides.[26] These molecules form the building blocks that give access to a collection of peripherally functionalized foldamers. A high-yielding synthetic methodology is described for the introduction of OPV3 and OPV4 chromophores. Both chromophores possess chiral alkyl tails to allow circular dichroism (CD) spectroscopy studies, and an additional gallic acid derived moiety guarantees solubility in most common organic solvents.

Results and Discussion

Design and Synthesis. Target poly(ureidophthalimide)s decorated with OPV3 (**3a**) and OPV4 (**3b**) were obtained by reaction of 3,6-diaminophthalimides **1a**,**b**[26] with the corresponding diisocyanates **2a**,**b** in refluxing toluene in the presence of *p*-dimethylaminopyridine (DMAP) (Scheme 1).

Monomers **1a**,**b** are synthesized starting by reaction of 3,6-bis(acetylamino)phthalic anhydride **4** with primary amines **5a**,[27]**b**[28] in refluxing dioxane for 17 h, which gives 3,6-bis(acetylamino)phthalimides **6** (Scheme 2).[26] Subsequent amide hydrolysis of **6** in the presence of aqueous HCl in refluxing dioxane furnishes 3,6-diaminophthalimides **1a**,**b**,[26] which can be quantitatively converted into the corresponding diisocyanates **2a**,**b** by exposure to a 20 wt % solution of phosgene in toluene.

After polymerization, column chromatography on silica gel with a gradient of chloroform to 10 v% ethyl acetate in chloroform easily removes the nonmigrating DMAP and allows separation of the longer from the shorter oligomers. The first fraction **3aI** contains oligomers of approximately 6−25 units (66 wt %), whereas the second fraction **3aII** consists of oligomers with lengths between 2 and 7 units (15 wt %) based on GPC analysis (Figure 2). Although ^{1}H NMR end-group analysis has proven a most reliable method to estimate the average oligomeric length, we found that GPC is more useful in this case since the broad and overlapping signals in ^{1}H NMR hamper proper end-group analysis.[29] Moreover, ^{1}H NMR gives the average length, whereas GPC gives more information on the total distribution.

A similar separation on polymeric distribution **3b** gave longer OPV4-decorated ureidophthalimide oligomers **3bI** with lengths ranging from 5 to 21 units (61 wt %) and shorter oligomers

(12) Huc, I. *Eur. J. Org. Chem.* **2004**, 17−29.
(13) Zhang, A.; Han, Y.; Yamato, K.; Zeng, X. C.; Gong, B. *Org. Lett.* **2006**, *8*, 803−806.
(14) Corbin, P. S.; Zimmerman, S. C.; Thiessen, P. A.; Hawryluk, N. A.; Murray, T. J. *J. Am. Chem. Soc.* **2001**, *123*, 10475−10488.
(15) Van Gorp, J. J.; Vekemans, J. A. J. M.; Meijer, E. W. *Chem. Commun.* **2004**, 60−61.
(16) Sinkeldam, R. W.; van Houtem, M. H. C. J.; Pieterse, K.; Vekemans, J. A. J. M.; Meijer, E. W. *Chem.−Eur. J.* **2006**, *12*, 6129−6137.
(17) Katayama, H.; Kooijmans, H.; Vekemans, J. A. J. M.; Meijer, E. W. Unpublished results.
(18) Maurizot, V.; Linti, G.; Huc, I. *Chem. Commun.* **2004**, 924−925.
(19) (a) Goto, K.; Moore, J. S. *Org. Lett.* **2005**, *7*, 1683−1686. (b) Stone, M. T.; Moore, S. J. *Org. Lett.* **2004**, *6*, 469−472. (c) Tanatani, A.; Hughes, T. S.; Moore, J. S. *Angew. Chem., Int. Ed.* **2002**, *41*, 325−328. (d) Prince, R. B.; Barnes, S. A.; Moore, J. S. *J. Am. Chem. Soc.* **2000**, *122*, 2758−2762.
(20) Garric, J.; Léger, J. M.; Huc, I. *Angew. Chem., Int. Ed.* **2005**, *44*, 1954−1958.
(21) Hou, J. L.; Shao, X. B.; Chen, G. J.; Zhou, Y. X.; Jiang, X. K.; Li, Z. T. *J. Am. Chem. Soc.* **2004**, *126*, 12386−12394.
(22) Recent reviews: (a) Segura, J. L.; Martin, N.; Guldi, D. M. *Chem. Soc. Rev.* **2005**, *34*, 31−47. (b) Hoppe, H.; Sariciftci, N. S. *J. Mater. Res.* **2004**, *19*, 1924−1945.
(23) Recent reviews: (a) Horowitz, G. *Adv. Mater.* **1998**, *10*, 365−377. (b) Dodabalapur, A.; Katz, H. E.; Torsi, L. *Adv. Mater.* **1996**, *8*, 853−855. (c) Sun, Y.; Liu, Y.; Zhu, D. *J. Mater. Chem.* **2005**, *15*, 53−65. (d) Kraft, A. *Chem. Phys. Chem.* **2001**, *2*, 163−165.
(24) A selection: (a) Hoeben, F. J. M.; Herz, L. M.; Daniel, C.; Jonkheijm, P.; Schenning, A. P. H. J.; Silva, C.; Meskers, S. C. J.; Beljonne, D.; Phillips, R. T.; Friend, R. H.; Meijer, E. W. *Angew. Chem., Int. Ed.* **2004**, *43*, 1976−1979. (b) Ajayaghosh, A.; George, S. J.; Praveen, V. K. *Angew. Chem., Int. Ed.* **2003**, *42*, 332−335. (c) Schenning, A. P. H. J.; Jonkheijm, P.; Peeters, E.; Meijer, E. W. *J. Am. Chem. Soc.* **2001**, *123*, 409−416.
(25) A selection: (a) Wolffs, M.; Hoeben, F. J. M.; Beckers, E. H. A.; Schenning, A. P. H. J.; Meijer, E. W. *J. Am. Chem. Soc.* **2005**, *127*, 13484−13485. (b) Schenning, A. P. H. J.; van Herrikhuyzen, J.; Jonkheijm, P.; Chen, Z.; Würthner, F.; Meijer, E. W. *J. Am. Chem. Soc.* **2002**, *124*, 10252−10253. (c) Beckers, E. H. A.; van Hal, P. A.; Schenning, A. P. H. J.; El-Ghayoury, A.; Peeters, E.; Rispens, M. T.; Hummelen, J. C.; Meijer, E. W.; Janssen, R. A. J. *J. Mater. Chem.* **2002**, *12*, 2054−2060.
(26) Sinkeldam, R. W.; van Houtem, M. H. C. J.; Koeckelberghs, G.; Vekemans, J. A. J. M.; Meijer, E. W. *Org. Lett.* **2006**, *8*, 383−385.
(27) The synthesis of **5a** (OPV3−NH_2) will be published elsewhere.
(28) (a) Peeters, E.; van Hal, P. A.; Meskers, S. C. J.; Janssen, R. A. J.; Meijer, E. W. *Chem.−Eur. J.* **2002**, *8*, 4470−4474. (b) Syamakumari, A.; Schenning, A. P. H. J.; Meijer, E. W. *Chem.−Eur. J.* **2002**, *8*, 3353−3361.
(29) Dolain, C.; Grelard, A.; Laguerre, M.; Jiang, H.; Maurizot, V.; Huc, I. *Chem.−Eur. J.* **2005**, *11*, 6135−6144.

Scheme 1. Synthesis of Ureidophthalimide Foldamers Decorated with OPV3 (**3a**) and OPV4 (**3b**)[a]

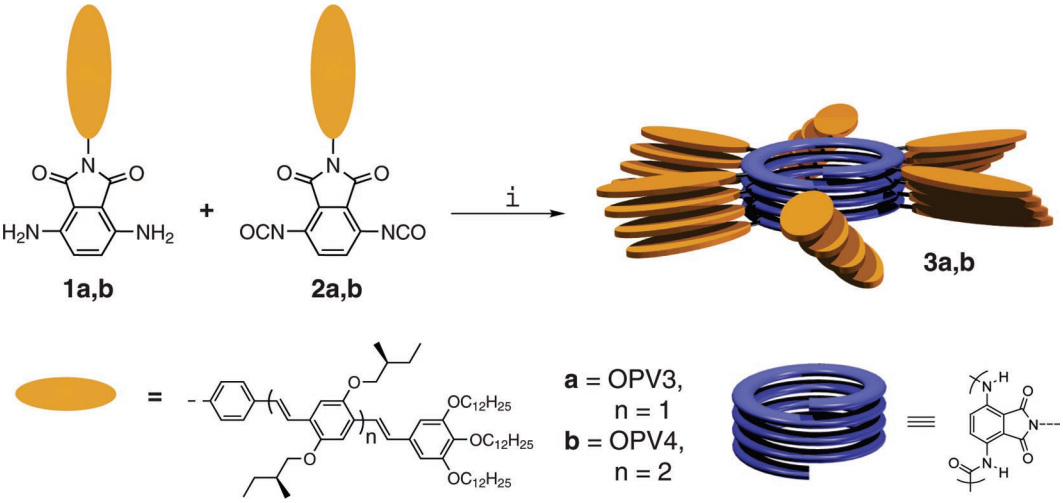

[a] (i) DMAP (1.0 equiv), $PhCH_3$, reflux, 17 h.

Scheme 2. Synthesis of Polymer Precursors **1a**,**b**[26] and **2a**,**b**[a]

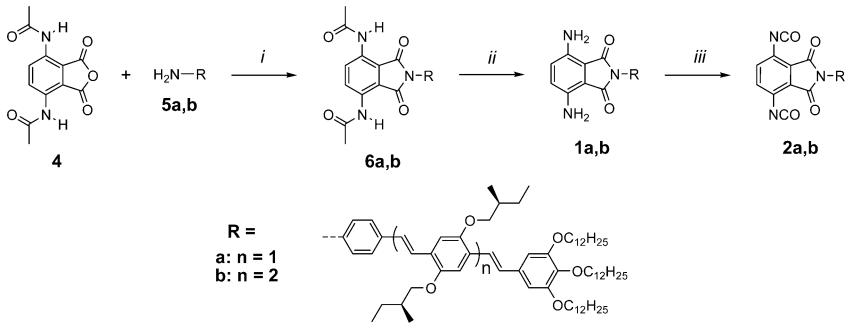

[a] (i) Dioxane, reflux, 17 h. **6a**: 91%, **6b**: 87%. (ii) HCl aqueous in dioxane, reflux, 4 h. **1a**: 81%, **1b**: 75%. (iii) $COCl_2$ (20 equiv), $PhCH_3$, rt to reflux, ~100%.

3bII with lengths of 1−5 units (7 wt %).[30] This demonstrates that separation over silica gel is a facile method to remove the shorter oligomers. Model studies and scanning tunneling microscopy (STM) data published below have shown that approximately 7−9 units may complete one turn.[31] This means that oligomeric lengths shorter than seven units will presumably not contribute to the folding.

UV−Vis and CD Spectroscopy of 3aI (OPV3). The nature of the solubilizing π-conjugated peripherals enables UV−vis and CD spectroscopic studies in various solvents. Thus, **3aI** is subjected to a study in $CHCl_3$, THF, and heptane (Figure 3). A solution in chloroform of **3aI** displays two absorption maxima in the UV−vis spectrum located at 323 nm (ϵ = 38 700 M^{-1} cm^{-1}) and 405 nm (ϵ = 47 800 M^{-1} cm^{-1}), which can be attributed to the ureidophthalimide moiety and the OPV3 unit, respectively. This solution proved to be CD silent, suggesting an achiral conformation for the oligomers or a conformation that lacks a preferred chiral orientation of the OPV side chains. When the solution in $CHCl_3$ was concentrated and the sample was redissolved in heptane again, no Cotton effect was observed although in the UV−vis spectrum a slight red shift of 6 nm was observed for the first maximum to 329 nm (ϵ = 30 600 M^{-1} cm^{-1}) and a hypsochromic shift for the highest wavelength absorption to 401 nm (ϵ = 37 500 M^{-1} cm^{-1}). Both shifts are indicative for $\pi-\pi$ stacking of the OPV units.[32] When the solution in $CHCl_3$ was concentrated and redissolved in THF, two CD effects were observed, of which the first was located at 328 nm ($g = -5.0 \times 10^{-4}$) and the second displayed a bisignate Cotton effect with a zero crossing at 399 nm and maxima at 379 nm ($g = +4.4 \times 10^{-4}$) and 416 nm ($g = -3.8 \times 10^{-4}$). The zero crossing of this bisignate CD effect coincides with the highest absorption maximum in the UV−vis spectrum at 398 nm (ϵ = 43 700 M^{-1} cm^{-1}). This absorption can be attributed to the $\pi-\pi^*$ transition of the OPV3 unit, implying a chiral stacking of the OPV3 moieties. It is important to mention that 3,6-bis(acetylamino)-*N*-OPV3-phthalimide (**6a**),[26] the precursor for diamino monomer **1a**, shows no Cotton effect in THF or $CHCl_3$. Moreover, THF is known to be a good solvent for isolated OPV3 chromophores, and thus aggregation is not expected. Furthermore, the negative exciton coupling of the bisignate Cotton effect suggests the presence of a left-handed helical arrangement of the transition dipoles of the OPV units.[33,34] In contrast to the measurement in heptane with a chloroform history, the measurement in heptane with a THF history does show a Cotton effect. This most remarkable

(30) GPC traces of OPV4-decorated oligo(ureidophthalimide) fractions **3bI** and **3bII** are included in the Supporting Information.
(31) van Gorp, J. J. Helices by Hydrogen Bonding. Ph.D. Thesis, Eindhoven University of Technology, Eindhoven, The Netherlands, 2004.
(32) Schenning, A. P. H. J.; Jonkheijm, P.; Peeters, E.; Meijer, E. W. *J. Am. Chem. Soc.* **2001**, *123*, 409−416.
(33) Jonkheijm, P.; Hoeben, F. J. M.; Kleppinger, R.; van Herrikhuyzen, J.; Schenning, A. P. H. J.; Meijer, E. W. *J. Am. Chem. Soc.* **2003**, *125*, 15941−15949.
(34) Davydov, A. S. *Zh. Eksp. Teor. Fiz.* **1948**, *18*, 210−218.

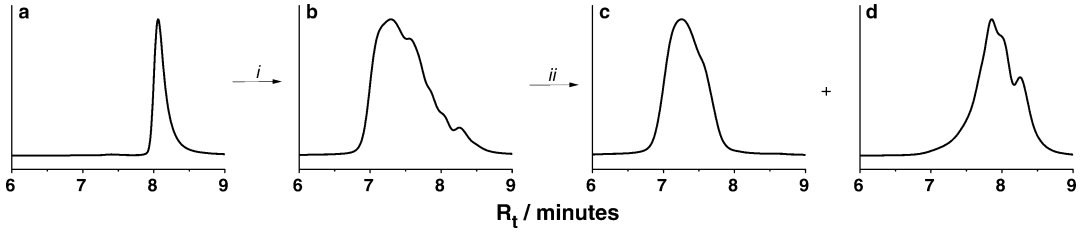

Figure 2. GPC analysis of (a) monomer **1a**, (b) crude polymer **3a**, (c) long oligomers fraction **3aI**, and (d) short oligomers fraction **3aII**. GPC is measured in $CHCl_3$ (UV detection at 420 nm) mixed-D column and polystyrene as internal standard.

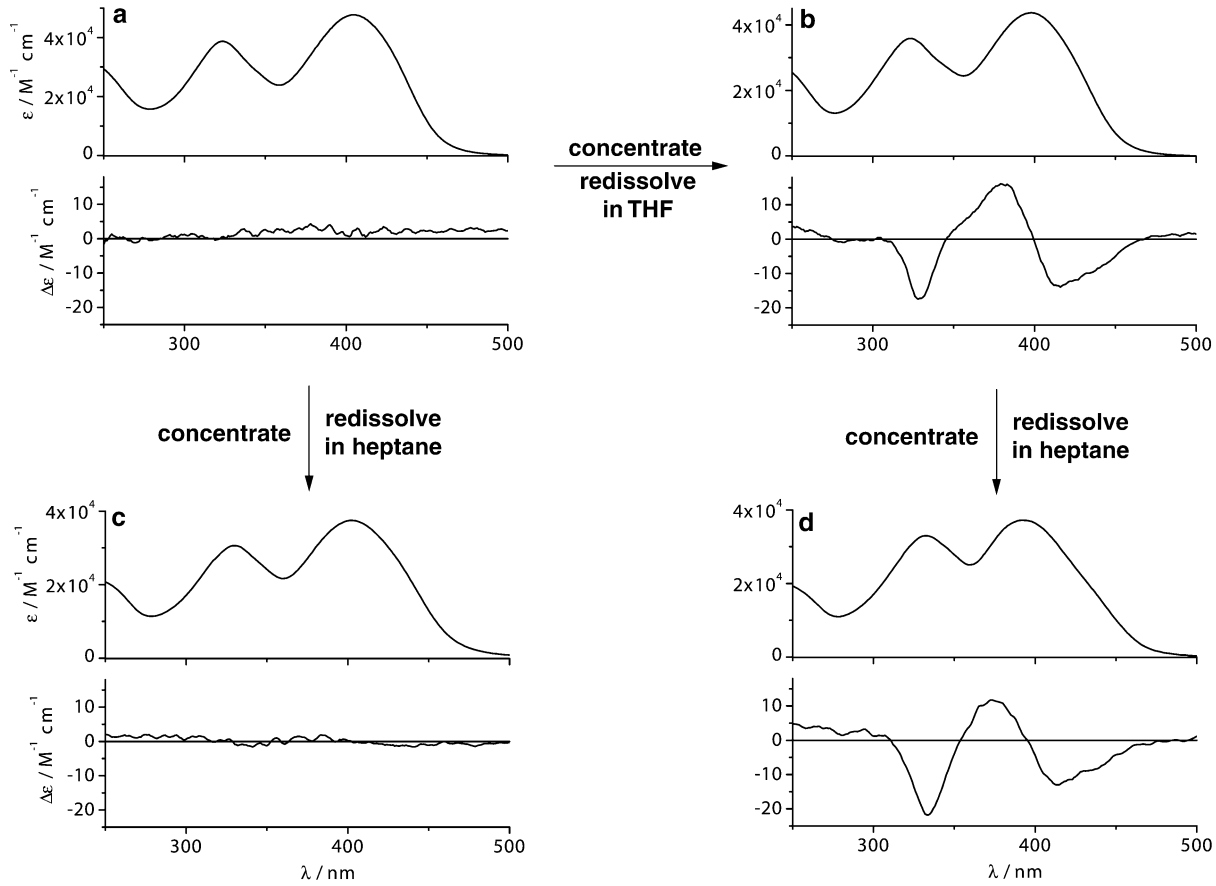

Figure 3. UV−vis and CD spectra of longer oligomers fraction **3aI** in (a) $CHCl_3$, 2.4×10^{-5} M, (b) THF, 2.9×10^{-5} M, (c) heptane, 2.1×10^{-5} M with a $CHCl_3$ history, and (d) heptane 2.3×10^{-5} M with a THF history.

observation implies the preservation of the secondary architecture in the solid phase during concentration from THF and its retention when subsequently redissolved in heptane. The maximum of the first Cotton effect in heptane is located at 333 nm ($g = -6.6 \times 10^{-4}$). The zero crossing of the bisignate Cotton effect underwent a minor blue shift and is now positioned at 395 nm with maxima at 373 nm ($g = +3.8 \times 10^{-4}$) and 413 nm ($g = -4.2 \times 10^{-4}$). The same blue shift is observed for the absorption maximum of the OPV3 unit in the UV−vis spectrum now located at 392 nm ($\epsilon = 37\,200$ M^{-1} cm^{-1}). Furthermore, a small bathochromic shift to 333 nm ($\epsilon = 33\,000$ M^{-1} cm^{-1}) is observed for the short wavelength absorption. Another fascinating feature of this system is the fact that the CD effect is lost upon concentration of the solution in heptane and redissolution of the solid in chloroform. However, concentration of the latter and redissolution in THF regenerate the Cotton effect. This cycle can be repeated without observable changes in the UV−vis and CD spectra. Seemingly THF is capable of forming a chiral secondary architecture that can be transferred to heptane but is "erased" in chloroform. In addition to the remarkable CD results, the UV−vis measurement clearly shows a significantly lower (∼20%) molar absorption coefficient for the long wavelength absorption of **3aI** in heptane compared to that in $CHCl_3$ and THF. This hypochromic (decrease in absorption intensity) effect is an indication for tight $\pi-\pi$ stacking that is also observed in DNA and π-stacked polymers.[35,36]

Above all, these experiments demonstrate that heptane is not capable of inducing nor disrupting a chiral secondary architecture but rather dissolves a preformed aggregate. This is in agreement with temperature-dependent CD measurements in THF and heptane (Figure 4). The gradually decreasing Cotton effect in THF upon increasing the temperature, which is reclaimed upon cooling, demonstrates the dynamics of the secondary architecture in THF. A melting curve could be constructed from the temperature-dependent Cotton effect at 415

(35) Nakano, T.; Yade, T. *J. Am. Chem. Soc.* **2003**, *125*, 15474−15484.
(36) Schuster, G. B. *Acc. Chem. Res.* **2000**, *33*, 253−260.

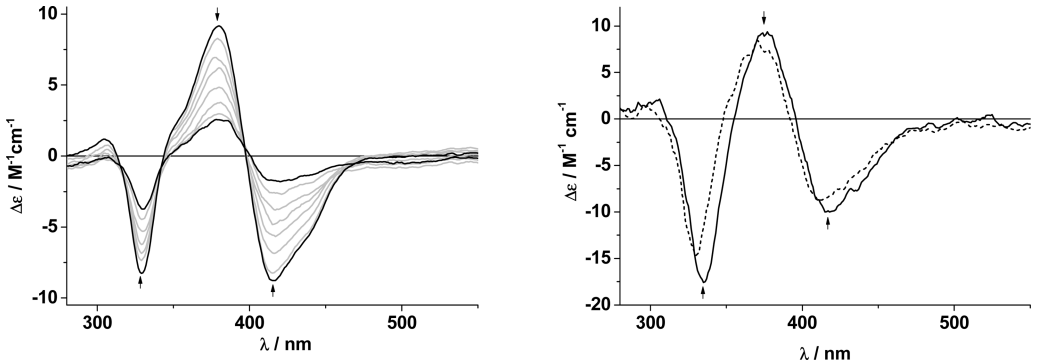

Figure 4. Temperature-dependent CD measurements of solution of **3aI** in (left) THF, 3.1×10^{-5} M from 20 °C (black line) in steps of 5 °C (gray lines) to 55 °C (black line) and (right) heptane, 3.2×10^{-5} M with a THF history at 20 °C (black line) and 85 °C (dashed line).

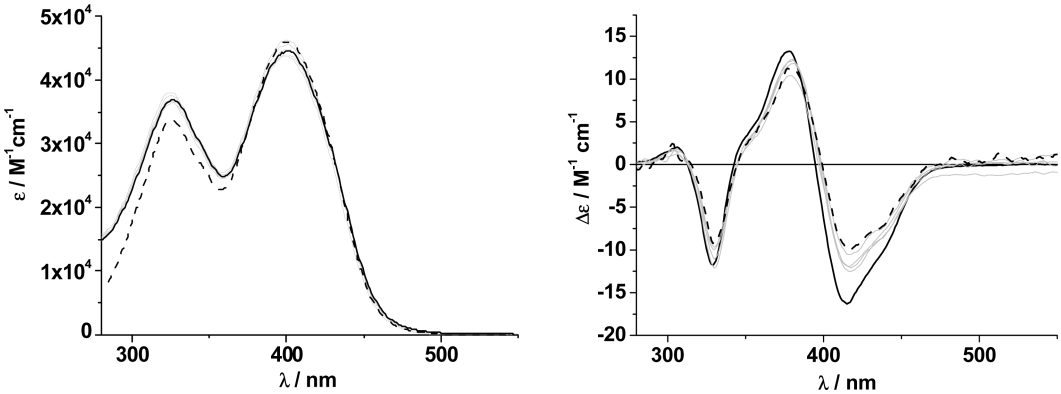

Figure 5. Concentration-dependent UV−vis (left) and CD (right) spectra of **3aI** in THF at 20 °C ranging from 5×10^{-4} M (solid black line) to 5×10^{-6} M (dashed black line) and intermediate steps (gray lines).

Table 1. IR Absorptions of **3aI**, NEAT from Different Solvents (ν in cm^{-1})

	urea–H	imid C═O	urea C═O
THF	3342	1727	1699
THF → heptane	3343	1728	1699
$CHCl_3$	3347	1724	1696
$CHCl_3$ → heptane	3347	1724	1696

nm in THF and is depicted in Figure 8 (vide infra). This is in strong contrast to the temperature-dependent measurements in heptane that clearly show stability of the secondary architecture. Moreover, similar measurements in dodecane under prolonged heating at 100 °C hardly altered the Cotton effect.

The UV−vis spectra of **3aI** in THF at concentrations ranging from 5×10^{-4} to 5×10^{-6} M display no differences in the position nor in the intensity of the absorption maxima. Despite the minor changes, the concentration-dependent CD spectra of **3aI** in THF at 20 °C reveal an almost concentration-independent Cotton effect (Figure 5). This suggests that the Cotton effect is the result of an intramolecular organization of the OPV3 chromophores and that interfoldamer aggregation is not responsible for the chirality in the concentration range between 5×10^{-4} and 5×10^{-6} M.[37]

To get more insight into the typical urea N−H, C═O, and imide C═O vibrations, solid phase infrared (IR) spectra of **3aI** from different solvents have been collected (Table 1). The measurements clearly reveal that films of **3aI** drop cast from THF and heptane with a THF history give the same values. But the values differ from drop cast films of **3aI** from $CHCl_3$ and heptane with a $CHCl_3$ history solution. Although the differences are small, the results are in agreement with the CD spectroscopy results in the sense that both solvents induce a different secondary organization affecting the urea conformation. However, for all solvents the IR spectra indicate strong hydrogen bonding for the urea hydrogens[38] and, hence, a cisoid urea conformation. This is in full agreement with the molecular modeling[16] and X-ray structure[17] of a dimer. Therefore, the differences in $CHCl_3$, THF, and heptane are the result of subtle organizational effects of both the backbone and the periphery. These results imply that, despite the absence of a Cotton effect in solution, a complete unfolding in $CHCl_3$ is unlikely.

A final subjective but noteworthy remark is the observation that solubilizing **3aI** in heptane seemed to be easier from a sample with a THF history than from one with a $CHCl_3$ history. This can be rationalized by considering the putative helical organization in THF that shields the relatively polar ureidophthalimide core from the apolar heptane. However, this is not the case when **3aI** has a chloroform history in which there is no such shielding effect of the polar core due to folding. Solvents with similar hydrogen bond accepting capabilities might harvest the same effect. Although dioxane solution is structurally related to THF, CD analysis of a dioxane solution of **3aI** with a $CHCl_3$ history reveals no Cotton effect. Measuring a dioxane solution with a THF history also did not display a Cotton effect. Although not explanatory, these results substantiate the unique role of THF in the folding process.

(37) Matthews, J. R.; Goldoni, F.; Schenning, A. P. H. J.; Meijer, E. W. *Chem. Commun.* **2005**, *44*, 5503−5505.

(38) Versteegen, R. M.; Sijbesma, R. P.; Meijer, E. W. *Macromolecules* **2005**, *38*, 3176−3184.

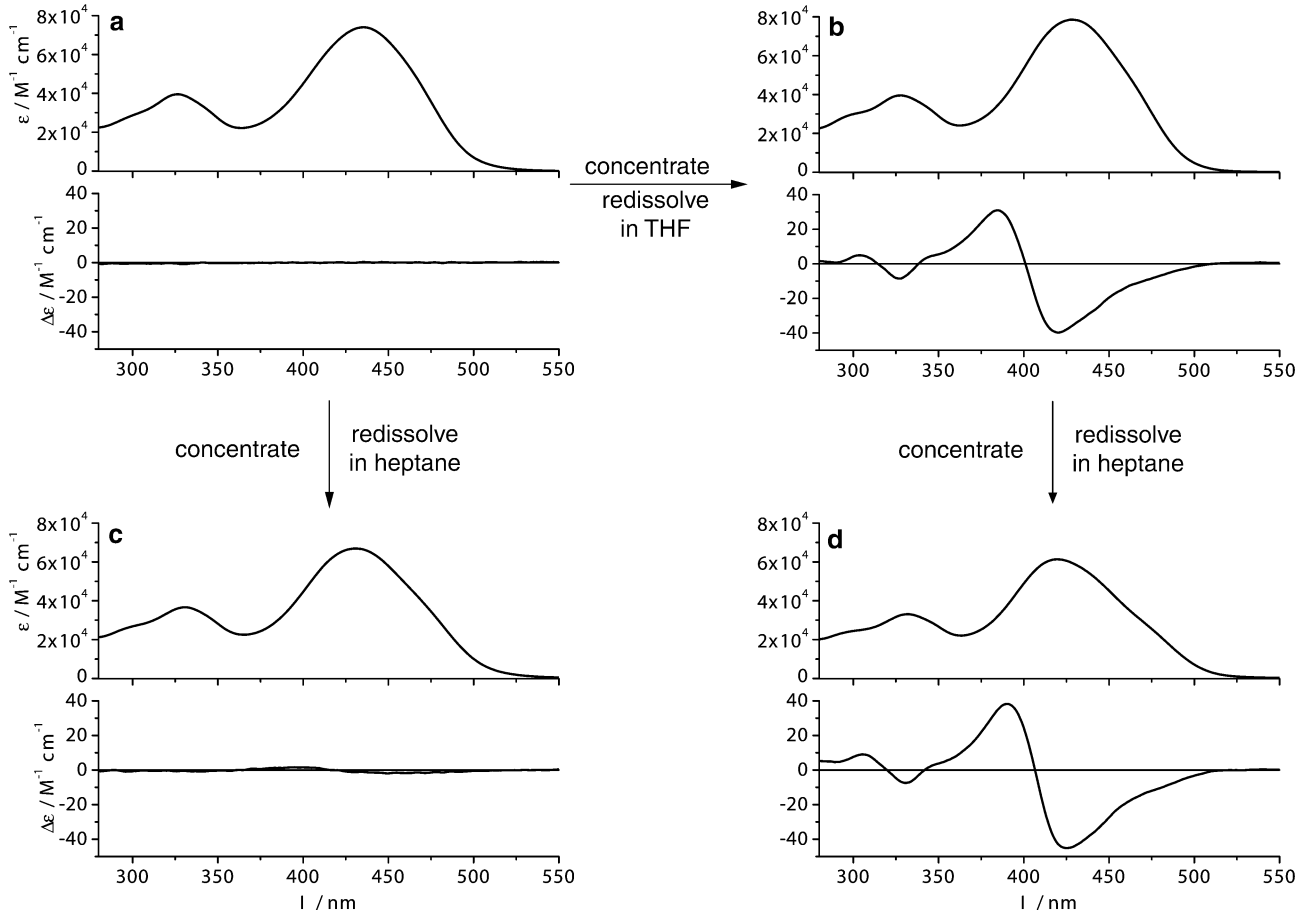

Figure 6. UV−vis and CD spectra of **3bI** in (a) $CHCl_3$, 1.3×10^{-5} M, (b) THF, 1.5×10^{-5} M, (c) heptane, 1.4×10^{-5} M with a $CHCl_3$ history, and (d) heptane 1.4×10^{-5} M with a THF history.

It is tempting to assume that THF induces or at least facilitates the folding process. It has been previously reported that especially diphenyl ureas substituted with electron-withdrawing groups in the meta position are prone to cocrystallization with hydrogen-bonding acceptors such as THF.[39] Furthermore, therein it is stated that hydrogen-bonding acceptor groups in ortho position may form intramolecular hydrogen bonds with the urea protons which themselves prefer an anti relationship to the urea carbonyl. The combination of the above-described interactions may induce a curvature that eventually nucleates folding in poly(ureidophthalimide)s. Further evidence for this statement is given below (in STM Analysis of Shorter Oligomers).

UV−Vis and CD Spectroscopy of 3bI (OPV4). Fraction **3bI** (longer oligomers decorated with OPV4 units) was subjected to a similar photophysical study in $CHCl_3$, THF, and heptane. The remarkable "memory" effect reported for the OPV3-decorated poly(ureidophthalimide) **3aI** (Figure 3) was also observed for the OPV4 analogue **3bI**. Also in this system it was possible to induce the secondary structure in THF, preserve it in heptane, and "erase" it in chloroform. This cycle could be repeated without noticeable changes in the UV−vis and CD spectra. The UV−vis spectrum of a solution in $CHCl_3$ shows two absorption maxima located at 326 nm ($\epsilon = 39\,500$ M^{-1} cm^{-1}) and 436 nm ($\epsilon = 74\,000$ M^{-1} cm^{-1}), which can be attributed to the ureidophthalimide moiety and the OPV4 unit, respectively (Figure 6). Furthermore, **3bI** proved to be CD silent in $CHCl_3$, suggesting a random coil conformation. The UV−vis spectrum of **3bI** in THF shows absorption maxima at 328 nm ($\epsilon = 39\,600$ M^{-1} cm^{-1}) and 429 nm ($\epsilon = 78\,500$ M^{-1} cm^{-1}).

The solution in THF reveals two bisignate Cotton effects: the first at 304 nm ($g = +1.6 \times 10^{-4}$) and 328 nm ($g = -2.1 \times 10^{-4}$) with a zero crossing at 314 nm and a second bisignate Cotton effect at 385 nm ($g = +8.9 \times 10^{-4}$) and 420 nm ($g = -5.2 \times 10^{-4}$) with a zero crossing at 401 nm. This is a strong indication for the chiral organization of the OPV4 chromophores. It is unclear why the zero crossing does not coincide with the absorption maximum in UV−vis as was observed for the OPV3 foldamer (Figure 2). Moreover, in contrast to the CD measurements on the OPV3 system, this system also shows a bisignate Cotton effect in the short wavelength regime which can be attributed to a chiral arrangement of the phthalimide units. A solution in heptane with a $CHCl_3$ history is CD silent with somewhat shifted maxima at 330 nm ($\epsilon = 36\,700$ M^{-1} cm^{-1}) and 430 nm ($\epsilon = 66\,900$ M^{-1} cm^{-1}), compared to the UV−vis measurement in $CHCl_3$. However, a solution in heptane with a THF history reveals two bisignate Cotton effects. The short wavelength bisignate Cotton effect has a zero crossing at 320 nm and maxima at 305 nm ($g = +3.6 \times 10^{-4}$) and 331 nm ($g = -2.2 \times 10^{-4}$). The second bisignate effect has maxima at 390 nm ($g = +1.0 \times 10^{-3}$) and 425 nm ($g = -7.5 \times 10^{-4}$) with a zero crossing at 407 nm. The accompanying UV−vis spectrum shows a minor blue shift of the absorption maxima

(39) (a) Etter. M. C.; Urbañczyk-Lipkowska, Z.; Zia-Ebrahimi, M.; Panunto, T. W. *J. Am. Chem. Soc.* **1990**, *112*, 8415−8426. (b) Etter, M. C.; Panunto, T. W. *J. Am. Chem. Soc.* **1988**, *110*, 5896−5897.

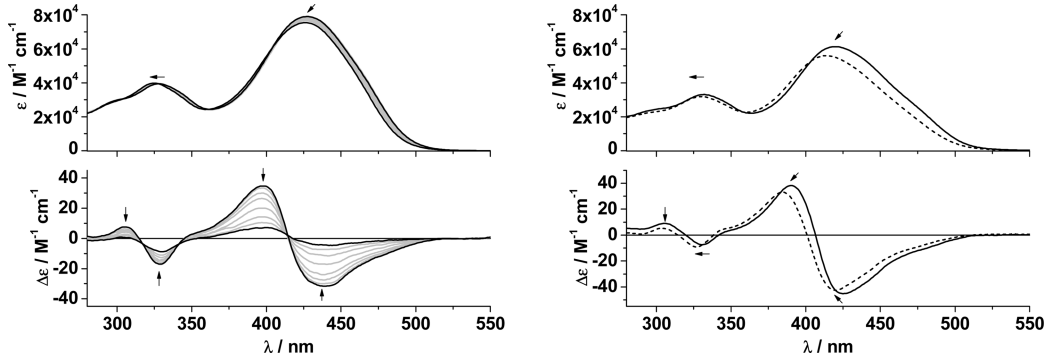

Figure 7. Temperature-dependent UV−vis and CD spectroscopy of **3bI** in (left) THF, 1.5×10^{-5} M, from 20 °C (black line) to 55 °C (black line) in steps of 5 °C (gray lines) and (right) heptane, 1.4×10^{-5} M, from 20 °C (black line) to 80 °C (dashed line).

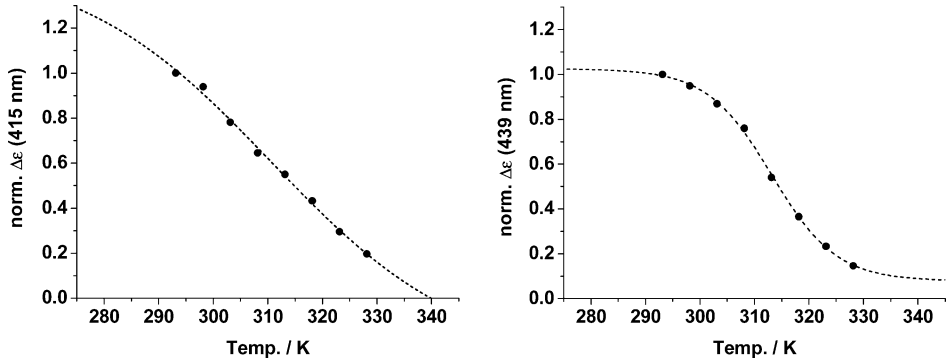

Figure 8. Melting curves of the Cotton effect in THF of **3aI** (OPV3-decorated, 3.1×10^{-5} M) at 415 nm (left) and of **3bI** (OPV4-decorated, 1.5×10^{-5} M) at 439 nm (right). The curves represent a sigmoidal fit (dashed line) of the data points (●).

to 332 nm ($\epsilon = 33\,100$ M^{-1} cm^{-1}) and 420 nm ($\epsilon = 61\,300$ M^{-1} cm^{-1}). In addition, monomeric precursor 3,6-bis(acetylamino)-*N*-OPV4-phthalimide (**6b**) is CD silent in $CHCl_3$, THF, and heptane.

The stability of the putative helical architectures is again investigated by subjecting solutions in THF and heptane of **3bI** to temperature-dependent UV−vis and CD experiments (Figure 7). Raising the temperature of the solution in THF hardly affects the intensity of the Cotton effect in combination with an almost negligible hypsochromic shift of the absorption maxima. The Cotton effect, however, does show a marked decrease upon raising the temperature, but reclaims its original value upon cooling and thereby demonstrates the dynamics of the system in THF.

However, elevating the temperature of the solution in heptane to 80 °C displays only a minor decrease of the Cotton effect, indicating the remarkable stability of the supramolecular architecture in heptane. Furthermore, it seems that the whole spectrum undergoes a shift to shorter wavelength. A similar effect is observed in the UV−vis spectrum. The nature of this effect remains unclear. In addition, prolonged heating of both solutions does not affect the Cotton effect any further.

Melting Curves of the Oligomers. Compared to the melting curve of **3aI** (decorated with OPV3) as recorded in THF, the melting curve of **3bI** (decorated with OPV4) in THF reveals a steeper slope, indicating a difference in the change in enthalpy involved in the unfolding process, albeit that the differences are small (Figure 8). The almost linear relationship between temperature and Cotton effect in **3aI** indicates the absence of a clear transition between folded and unfolded structures. The difference can be attributed to the larger π-surface in the case of the OPV4-decorated foldamer. The slope of the linear part of both curves and the melting transition (~312 K) are comparable. It must be noted that the Cotton effect in both cases does not reach zero, but the curve for OPV4-decorated foldamer hints to a more cooperative unfolding than for the OPV3-decorated foldamer. The stability of the folded chiral structures in heptane is too high to see the transition from an ordered helical state to a disordered state.

STM Analysis of Shorter Oligomers. To obtain experimental evidence for the curvature of the structures under investigation and hence to study their properties to arrive at a well-defined folded state, we investigated the short-chain fractions **3aII** (OPV3-decorated) and **3bII** (OPV4-decorated) containing chain lengths between two and seven repeat units with STM. Their organization on the solid−liquid interface of highly ordered pyrolytic graphite (HOPG) and 1-phenyloctane could be studied in detail with STM. Structural features appear in the STM images that reflect individual molecules. On the basis of the specific contrast of aromatic units (high tunneling efficiency) in the STM images, in combination with the distance analysis, we can correlate the bright rods with OPV units. Basically, two types of images were recorded. At first glance, in the sample containing OPV4-decorated ureidophthalimide oligomers (fraction **3bII**), the OPV4 rods appear mostly disordered (Figure 9a). Such images were also observed with a sample of **3aII**, containing OPV3-decorated ureidophthalimide oligomers (Figure 9c). The molecules are mobile as two images recorded sequentially never show an identical arrangement of the molecules (it takes ~10 s to record an image). Given the polydispersity of the sample, such a disordered arrangement is not surprising. As the intermolecular lateral interactions between the molecules are not optimized, the molecules are prone to in-plane (diffusional) and out-of-plane (desorption−adsorption)

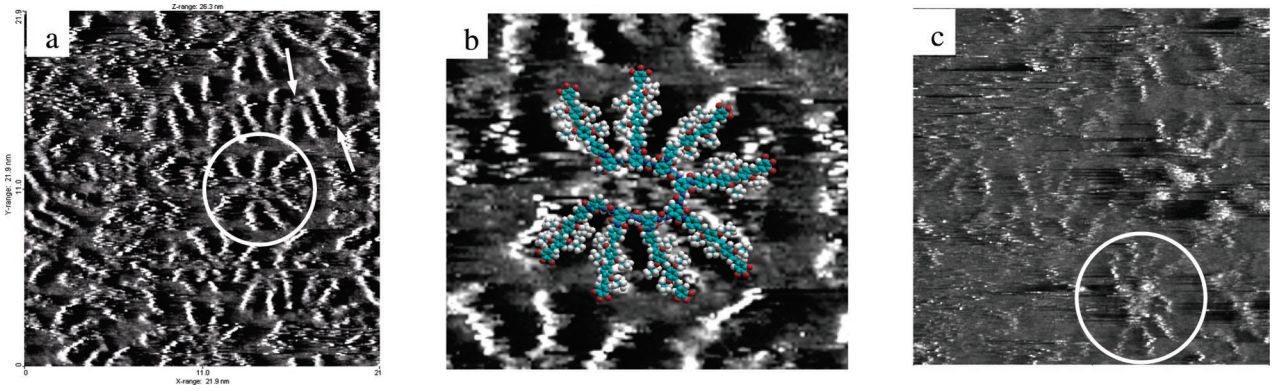

Figure 9. STM image of a random pattern of **3bII** at the 1-phenyloctane/graphite interface. (a) Noncalibrated image with a size of approximately 22 nm × 22 nm. $I_t = 0.80$ nA. $V_{bias} = -0.57$ V. The white arrows indicate dimers. Within the circle, a higher oligomer that could be an octamer is visible. (b) Zoom of the central area in part a, showing the octamer with a superimposed molecular model. (c) **3aII**, a circular structure of OPV3-decorated ureidophthalimide is depicted in the circle. Image size is 21 nm × 21 nm. $I_t = 0.79$ nA. $V_{bias} = -0.52$ V.

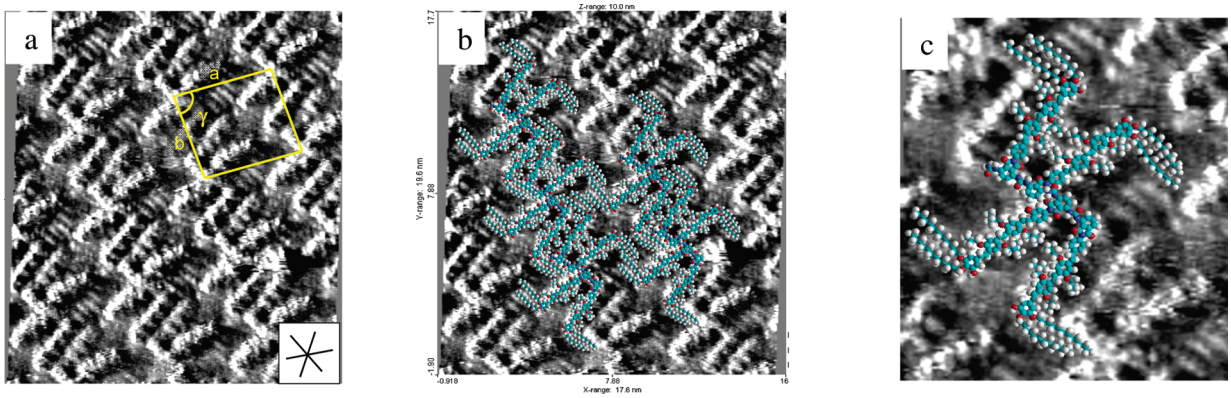

Figure 10. STM image of **3bII** at the 1-phenyloctane/graphite interface. (a) The unit cell is indicated in yellow. The lines in the inset at the lower right corner of the image indicate the direction of the major symmetry axis of graphite. Image size is 16.2 nm × 19.6 nm. $I_t = 0.80$ nA. $V_{bias} = -0.78$ V. (b) Some molecular models (dimers) superimposed on the STM image. (c) Zoom of STM image in part b with molecular model superimposed.

dynamic processes. In case of the OPV4-decorated ureidophthalimide oligomers, the image shows mainly dimer molecules indicated by white arrows (Figure 9a). The high abundance of dimers is in agreement with the GPC trace. In spite of the apparent random organization, both images clearly show higher homologues in a circular orientation as depicted by the white circle (Figure 9a,c). A superimposed model with all urea linkers in a cisoid conformation fits very well (Figure 9b). Exactly this shape is thought to be responsible for nucleation of folding in solution. Previously, a rosette organization based on intermolecular hydrogen bonding has been observed with OPV4 molecules equipped with a diamino triazine unit.[40]

In time, a second type of images appears for OPV4-decorated ureidophtahlimide oligomers, revealing a more regular arrangement of the molecules, locally leading to domains that are two-dimensionally crystalline (Figure 10). The two-dimensional arrangement can be described by a unit cell: $a = 5.2 \pm 0.1$ nm, $b = 4.3 \pm 0.1$ nm, $\gamma = 85 \pm 2°$, which contains four OPV rods. The submolecular contrast variation along the rods is attributed to the phenylene vinylene units. In addition to the bright rods, also alkyl chains are visible which run perpendicular to the OPV rods. Most likely, only two out of three dodecyloxy chains per OPV unit are adsorbed with their long molecular axis parallel to the substrate. Those adsorbed run (almost) parallel to one of the main symmetry axes of graphite which is frequently observed.

The formation of two-dimensional crystals is rather surprising given the polydispersity of the sample. It suggests that, in time, there is a selective adsorption of one given oligomer on the surface. On the basis of the image contrast and the analysis, it appears that tetramers with two cisoid and one transoid conformation or dimers with one cisoid conformation can give this regular packing. We cannot distinguish with absolute certainty between them. However, the molecular model of the tetramer underestimates the length of the "backbone" (2.4 nm), while in the case of dimers, the experimental distance (2.7 nm) fits the modeled one (2.6 nm) better. In addition, as the solution contains dimers in excess, it is also plausible to conclude that an excess of dimers will adsorb. The preferential adsorption of dimers is most likely driven by the thermodynamics of the adsorption−desorption process.

The study of the shorter oligomers on an HOPG surface substantiates the tendency of the OPV-decorated ureidophtalimides to adopt a curved and hence folded structure that can be attributed to the molecular design of the primary structure in which the intramolecular hydrogen bonding between the urea hydrogens and the adjacent imide carbonyls are highly directional in the folding process. This is in full agreement with the IR data, the molecular modeling, and the X-ray structure of a dimer. In contrast to the observation that short oligomers adopt

(40) (a) Miura, A.; Jonkheijm, P.; De Feyter, S.; Schenning, A. P. H. J.; Meijer, E. W.; De Schryver, F. C. *Small* **2005**, *1*, 131−137. (b) Jonkheijm, P.; Miura, A.; Zdanowska, M.; Hoeben, F. J. M.; De Feyter, S.; Schenning, A. P. H. J.; De Schryver, F. C.; Meijer, E. W. *Angew. Chem., Int. Ed.* **2004**, *43*, 74−78.

ordered structures on a surface, they do not lead to a Cotton effect in solution. This is due to their lack of length, being insufficient to form at least one turn, and hence the lack of $\pi-\pi$ interactions to secure the formation of stable secondary structures. However, the STM data of the short length oligomers support the proposal that the longer oligomers/polymers adopt a folded helical conformation that is dynamic in THF and stable in heptane and not present in $CHCl_3$.

Conclusions

In summary, we have shown that a poly(ureidophthalimide) backbone decorated with OPV chromophores assumes a random coil conformation in $CHCl_3$ but adopts a putative helical conformation in THF. Measurements in heptane show that the initial secondary organization is preserved depending on the solvent used prior to heptane. Moreover, temperature-dependent CD studies establish the dynamics of the secondary architectures in THF and the remarkable stability in heptane. We are certain that the intramolecular hydrogen bonding of the phthalimide units is responsible for the initial chiral alignment of the OPV chromophores. However, the rather small Cotton effects might be an indication of the presence of frustrated stacks due to nonchiral aggregation of OPV units.[41] Although the role of THF remains undefined, it is clear that solvent in general and THF specifically play an important role in the folding process. In contrast to the longer oligomers, the shorter oligomers do not seem to adopt a helical conformation in solution. However, STM analysis revealed the presence of circular architectures for OPV3 as well as OPV4 oligomers. The high abundance of dimers in the polydisperse sample resulted in the presence of a dense packing of dimers to maximize surface coverage. The various patterns observed on the graphite 1-phenyloctane interface are a logical result of the polydisperse nature of the sample.

Acknowledgment. We thank Ralf Bovee for GPC analysis, Dr. Albert Schenning for stimulating discussions, and Dr. Theresa Chang for the artwork. The Council of Chemical Science of the Dutch National Science Foundation (CW-NWO) is acknowledged for the financial support of the Dutch team. The authors in Leuven thank the Federal Science Policy through IUAP-V-03 and the Institute for the Promotion of Innovation by Science and Technology in Flanders (IWT). Financial support from the Fund for Scientific Research-Flanders (FWO) and K.U. Leuven is also acknowledged.

Supporting Information Available: GPC traces of OPV4-decorated ureiodophthalimide oligomers **3bI** and **3bII**. Experimental details concerning the synthesis of compounds **2a**, **2b**, **3a**, and **3b** and their characterization by ^{1}H-, ^{13}C NMR, and IR. This material is available free of charge via the Internet at http://pubs.acs.org.

JA063405D

(41) Schenning, A. P. H. J.; Jonkheijm, P.; Peeters, E.; Meijer, E. W. *J. Am. Chem. Soc.* **2001**, *123*, 409−416.